# An Integrated Model for the Cochlear Microphonic

Mohammad Ayat, Paul Teal,[a)] and Mark McGuinness

*Victoria University of Wellington,*

*P.O. Box 600,*

*Wellington 6140,*

*New Zealand*

(Dated: November 12, 2012)

**Abstract**

The cochlear microphonic (CM) is an electrical signal generated in the cochlea in response to sound. These electrical signals reflect mechanical activity in the cochlea and the excitation process of generating them. In other words, like other electrical vital signs such as the Electrocardiogram (ECG) and the Electroencephalogram (EEG), knowledge of how the CM is generated can allow its interpretation to be used as a diagnostic tool for audiologists. The CM allows the functionality of the ear to be examined, particularly when screening the hearing of an infant or any person who cannot cooperate during behavioural testing. In addition, the CM can show which specific parts of the cochlea are damaged and do not work properly. However, the difficulty of obtaining this signal and simplicity of other methods such as Otoacoustic Emissions have discouraged the use of the CM as a tool for studying a number of cochlea functions. The CM can provide an extremely valuable technique for investigations in hearing research and it can also have viable clinical applications.

An integrated model of the cochlea is presented by which the discrepancy between basilar membrane and CM tuning curves can be explained. The results of the model also suggest that *Spontaneous Cochlear Microphonic* (SCOMIC) should exist in the cochlea. The existence of this spontaneous electrical signal has not been previously reported.

PACS numbers:

## I. INTRODUCTION

The CM is an AC signal which is similar to the acoustic stimulus signal and is referred to as the steady-state part of the Auditory Evoked Potential (AEP) (Pickles, 2008). These compound graded responses are generated through the mechanical and electrical activity of the cochlea. The CM has been known for more than eighty years, but difficulty of obtaining these very small signals and uncertainty in the generation process of them causes them to rarely be used as an indication of cochlear performance (Teal et al., 2011; Cheatham et al., 2011). Improvement in measuring techniques has permitted the reliable non-invasive recording of these signals (Masood et al., 2012; Poch-Broto et al., 2009) which traditionally have been recorded invasively through transtympanic electrocochleography.

Even though improvements in observation and measuring techniques can reveal much information about the CM, there are still some gaps between what can be measured and the actual cochlear function. Therefore modelling plays an essential role in developing a better understanding of the origin of this biopotential and its behaviour. The simple and widely used model of generating the CM is the *resistance microphone* model (Davis, 1965; Gelfand, 2010). In this model, the resting potentials of the cochlea are modelled by two batteries. The primary battery is in the hair cells, the accessory battery is in the stria vascularis, and the mechano-electrical transduction (MET) channels are modelled by variable electrical resistors. Accordingly, the current through the hair cells is modulated by the changing electrical resistances resulting from cilia deflection. These processes result in electrical potential changes which comprise the CM.

Furthermore a network model of the resistors and batteries has been used to simulate the generation and distribution of the cochlear potentials (Strelioff, 1973). The model can be enhanced by including details of the electrical properties of the organ of Corti. The electrical component values of a detailed model of a radial section of the organ of Corti have been measured heuristically based on actual measurements of potentials inside the cochlea (Dal-

[a)]Electronic address: paul.teal@vuw.ac.nz

los, 1983, 1984) . Although the generation of the CM was not directly addressed in these papers, the parameter values and their proposed detailed electrical configuration are suitable for modelling the CM. Recent experiments have shown that some previous measurements of the parameter values pertinent to outer hair cells (OHCs) were not accurate enough and revised values have been measured (Johnson et al., 2011).

In this work, an integrated detailed model of the electrical and mechanical properties of the cochlea is presented using these new physiological measurements. We also explain the discrepancy between basilar membrane and CM tuning curves based on the results of the model. In addition, we investigate the possibility of the existence of *Spontaneous Cochlear Microphonic* (SCOMIC) based on the model. The SCOMIC will be generated due to activity of hair cells in the generation sites of Spontaneous Otoacoustic Emission (SOAE) and this investigation is explained in detail in Sections II.B and IV.

The remainder of this paper is arranged as follows: The nonlinear electromechanical model is described in Section II; frequency and time domain analyses are presented in Sections III and IV and conclusions are given in Section V.

## II. MODELLING

Vibrations of the basilar membrane cause the stereocilia of the outer hair cells to deflect resulting in changing MET channel currents. The alternation of these nonlinear currents activate mechanical amplifiers which amplify low-level basilar membrane displacement and compress high-level basilar membrane displacements (Ashmore et al., 2010). Since these channels are embedded in the electrical network of the organ of Corti, changing their currents also produces changes in extracellular current flow and creates the CM (Cheatham et al., 2011). These currents and their nonlinear effects result in an active force on the basilar membrane and tectorial membrane. This system is referred to as the cochlear amplifier. For modelling purposes usually this amplification effect is a simplified to (nonlinear) active damping gain which is driven by basilar membrane and tectorial membrane displacement

and velocity and acts as an active force on mechanical parts (Elliott et al., 2007; Neely and Kim, 1986). In other models (Mistrík et al., 2009) the effect is analysed separately without considering physical links between acoustical, mechanical, fluid and electrical parts. Simplified versions of these physical links have been considered in some proposed models but investigating the CM was not the main objective of those models (Ramamoorthy et al., 2007; Liu and Neely, 2010). The mechanical part of our model is similar to to the well-known model of Neely and Kim (1986), which has been the basis of many other models (Liu and Neely, 2010). This model has been summarised in Fig. 1. For more details of each part, the reader is referred to (Liu and Neely, 2010). For integrity of our current work we repeat some of the equations from (Liu and Neely, 2010, 2009; Teal et al., 2011).

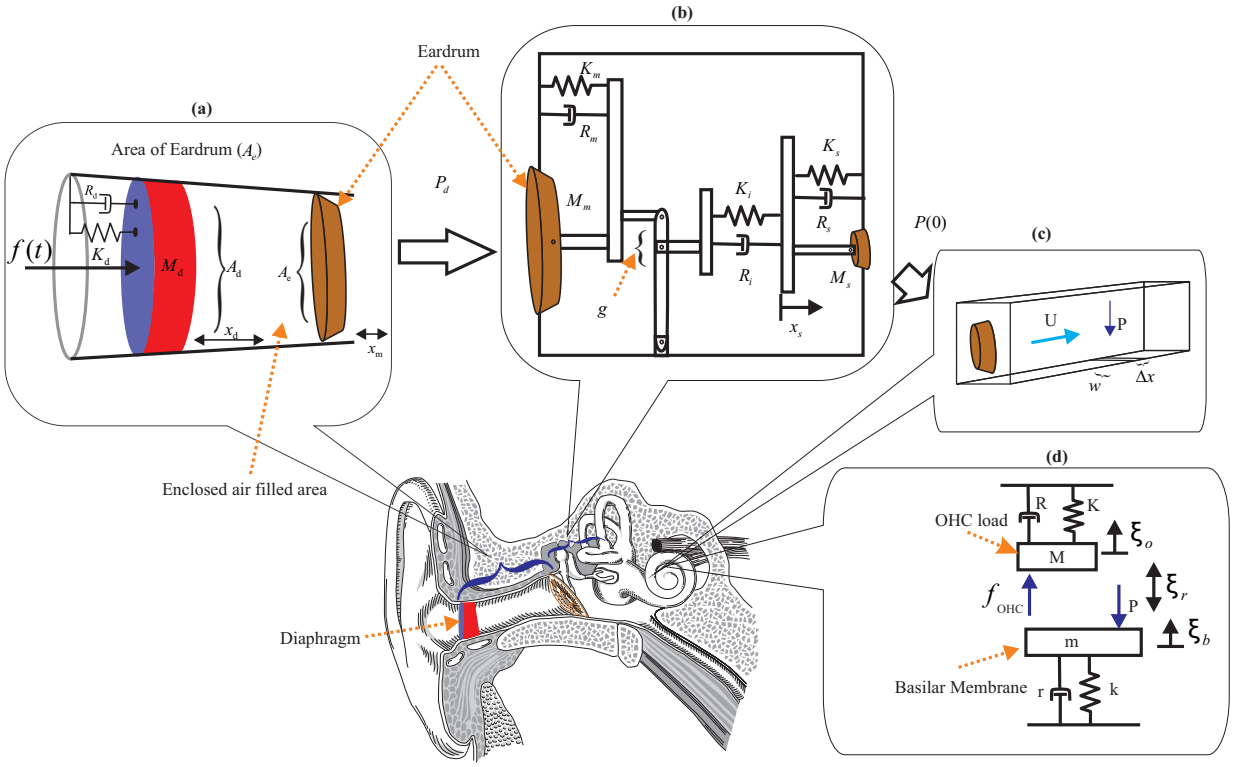


FIG. 1. (Liu and Neely, 2010)'s model. (a) shows the model of the ear canal. (b) shows the model of the middle ear (Redrawn with permission, from Liu and Neely (2010)) (c) shows the macromechanics model of the cochlea. (d) shows the micromechanics model of the cochlea.

## A. Cochlear Micromechanics

Cochlear micromechanics represents the mechanical and dynamic behaviour of a radial slice of the organ of Corti and the basilar membrane. The basilar membrane consists of transverse beamlike fibres (Iurato, 1962) having only weak longitudinal couplings, and hence for modelling purposes the organ of Corti can be divided into $N$ sections. Each section of micromechanical model consists of two parts representing the mass, stiffness and damping of the basilar membrane and OHC load respectively, as shown in Fig. 1(D), and the force ($f_{\mathrm{OHC}}$) which is induced by OHC Electromotility.

### *1. Mechano-electrical transduction current and electromotility*

Somatic contractions of OHCs are one of the mechanisms which have been put forward to explain the cochlear amplifier. This mechanism is activated by the MET current; details of this mechanism can be seen in (Dallos et al., 1996).

A Boltzmann function can be fitted to the MET current response to hair bundle displacement (Kennedy et al., 2005). In the present model, the MET current is described as a nonlinear antisymmetric saturating function of displacement and velocity of the reticular lamina (RL)(Liu and Neely, 2009). This nonlinear function is responsible for compression and amplification of the cochlear amplifier. Reduction in the length of the OHC accumulates charge $Q$ and OHC contraction displacement $\xi_o$ is linearly proportional to $Q$.

$$\xi_o = TQ \tag{1}$$

where $T$ is a piezoelectric constant. $Q$ is a Boltzmann function of

$$\tilde{V} = V_{\mathrm{OHC}} - Tf_{\mathrm{OHC}} \tag{2}$$

and $C_g = \partial Q/\partial \tilde{V}$. These equations are summarised in Fig. 2 (Liu and Neely, 2010)[1]. Displacement and velocity of both RL and OHC together with OHC and hair bundle voltages in each section of the organ of Corti construct a state vector as follows:

$$x_n = [\xi_{\mathrm{r}}, \dot{\xi}_{\mathrm{r}}, \xi_{\mathrm{o}}, \dot{\xi}_{\mathrm{o}}, V_{\mathrm{OHC}}, V_{\mathrm{HB}}]^{\top} \tag{3}$$

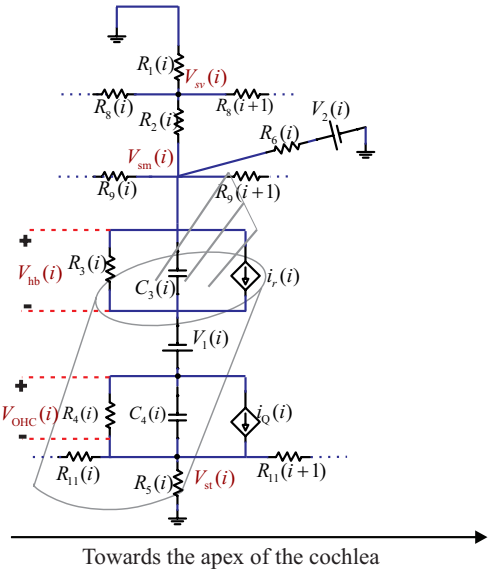


FIG. 2. OHC electrical model which is embedded in the electrical network of the organ of Corti. the MET channel current ($i_{\mathrm{r}}$) is a Boltzmann function of the displacement of the hair bundle i.e. $I(\eta) = \frac{I_{\max}}{2} \tanh \frac{2\eta}{I_{\max}}$ where $\eta = \alpha_{\mathrm{v}}\dot{\xi}_{\mathrm{r}} + \alpha_{\mathrm{d}}\xi_{\mathrm{r}}$ (Liu and Neely, 2010). $i_{\mathrm{Q}} = \frac{dQ}{dt}$ and from equation (1), $i_{\mathrm{Q}} = \dot{\xi}_o/T$ where $\dot{\xi}_o$ is the velocity of the OHC contraction. $V_{\mathrm{st}}$, $V_{\mathrm{sm}}$, $V_{\mathrm{sv}}$, $V_{\mathrm{OHC}}$ and $V_{\mathrm{HB}}$ are the potentials of the scalae tympani, media, vestibuli, and of the outer hair cells and hair bundles, respectively.

The set of $N$ state vectors (plus six more variables representing the state of the middle ear) creates a system with a $6N + 6$ length state vector $\mathbf{x}$. By considering a linearised version of the MET channel current ($i_{\mathrm{r}}$); the system can be represented in linear state-space form as follows[2]:

$$\dot{\mathbf{x}}(t) = \mathbf{A}\mathbf{x}(t) + \mathbf{B}\mathbf{u}(\mathbf{t}) \tag{4a}$$

$$\mathbf{y}(t) = \mathbf{C}\mathbf{x}(t) + \mathbf{D}\mathbf{u}(\mathbf{t}) \tag{4b}$$

Where

$$\mathbf{B}\mathbf{u}(\mathbf{t}) = [f(t),\, 0,\, \cdots,\, 0]^T$$

and $\mathbf{A}$ is a $(6N + 6) \times (6N + 6)$ state matrix and $f(t)$ is a stimulus force (see Fig. 1). The system output $\mathbf{y}(t)$ can be defined as any desired state variable. The $\mathbf{C}$ Matrix selects that

desired state variables and the **D** is the null matrix. The details of the formulations of **A** are reported in Appendix A.

### B. Stability

The stability of the system can be assessed by examining the eigenvalues of the state matrix **A**. Fig. 3 (a) and (b) show the locations of the roots of the linearised version of the model. There are no poles having positive real part and the system is stable. However inhomogeneities in physical parameters can make the system unstable (Elliott et al., 2007). In the current model, the stability of the model is very sensitive to positive feedback gains which result from OHCs motilities. Small perturbation in the gains of positive feedback along the cochlea can cause instability. Fig. 3 (b) and (d) demonstrate such perturbation and the resulting change in root locations, some of the poles have positive real part.

Although the nonlinearity in the MET channel current ($i_{\mathrm{r}}$) makes this system stable, this system still oscillates at frequencies corresponding to those poles on the right hand side of the origin in Fig. 3 (c) and (d). Each unstable pole can be considered as a source of SOAE (Ku et al., 2008). These mechanical oscillations are consequences of electrical oscillations, and accordingly, spontaneous cochlear microphonic (SCOMIC) will be generated due to these electrical activities of hair cells in the generation sites of SOAE. This phenomenon is discussed in Section IV.

## III. FREQUENCY ANALYSIS

The CM which is usually recorded from the round window using a transtympanic membrane electrode can be observed as the potential of the endolymphatic space above the basal hair cells ($V_{\mathrm{sm}}$ in Fig. 2)(Mistrík et al., 2009). Taking the Fourier transform of both sides of (4), the frequency response of output $\mathbf{y}(j\omega)$ can be calculated as:

$$\mathbf{y}(j\omega) = \mathbf{C}\,(j\omega\mathbf{I}\mathbf{A})^{-1}\mathbf{B}\,\mathbf{u}(j\omega) \tag{5}$$

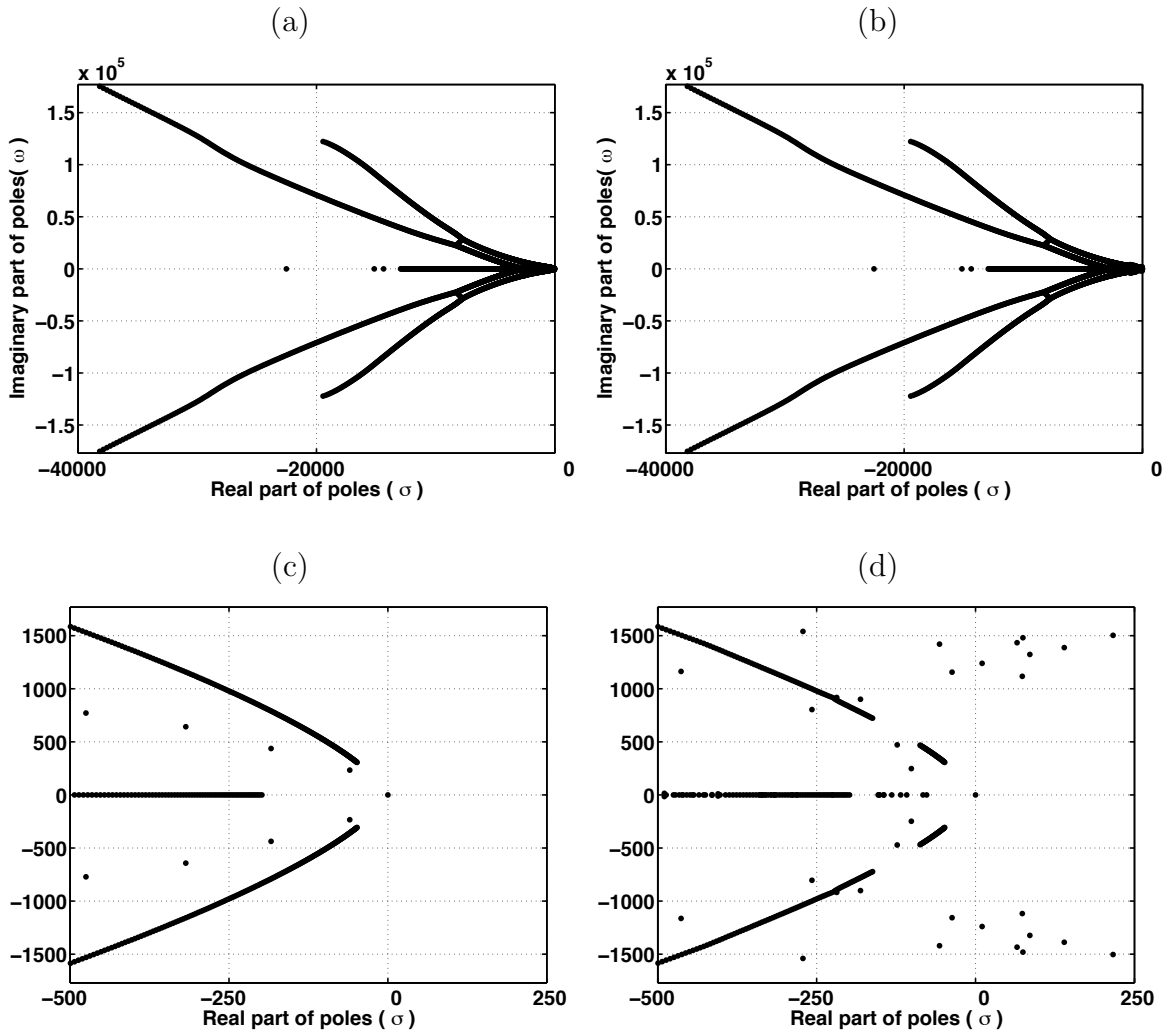


FIG. 3. Root locations of the combined system. (a) shows root locations of the linearised version of the model. (b) shows root locations of the system with small perturbations in the feedback gain. These perturbations are shown in Fig. 7. (c) and (d) are magnifications of (a) and (b) near the origin.

where matrix $\mathbf{C}$ extracts output variables of interest (in this case $V_{\mathrm{OHC}}$ and $V_{\mathrm{HB}}$). Other scalae potentials can be calculated using these two variables. Fig. 4 depicts the amplitudes of these potential variables as a function of the cochlear length. Despite the very similar amplitudes of these signals, they have a phase differences of $\pi$ near their peaks and nearly

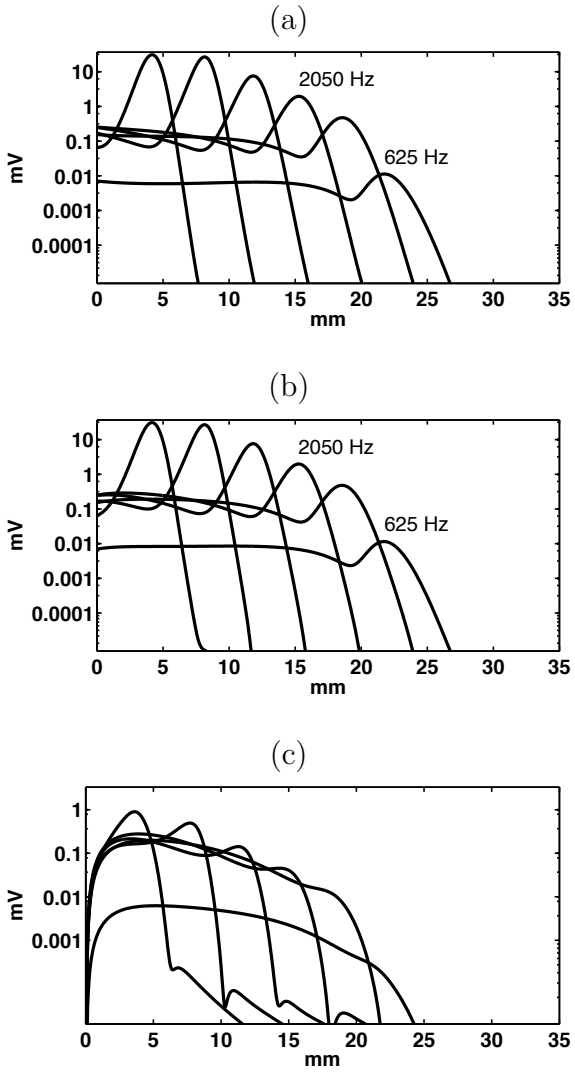


FIG. 4. (a), (b) and (c) illustrate amplitudes of $V_{\mathrm{OHC}}$, $V_{\mathrm{HB}}$ and $V_{\mathrm{OHC}} + V_{\mathrm{HB}}$ along the cochlea, respectively. Each graph shows the responses for six different stimulus frequencies: 625, 1150, 2050, 3700, 6700,12000 Hz

cancel each other (see Fig. 5). According to the model, the main reason of the broadness of the CM tuning curves is the phase difference of $\pi$ between $V_{\mathrm{OHC}}$ and $V_{\mathrm{HB}}$.

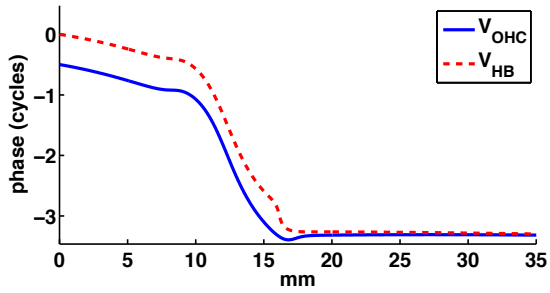


FIG. 5. Phase of $V_{\mathrm{OHC}}$ and $V_{\mathrm{HB}}$. For clarity, only curves with the Characteristic Frequency (CF)=3500 associated to the place 12.63 mm from the base in cochlea have been shown

## IV. TIME DOMAIN ANALYSIS

For frequency analysis, we used the linearised version of the model. However, in order to explore the nonlinear behaviour of the model, the model should be analysed in the time domain. One approach to time domain analysis is using the state-space representation of the model which forms a large system of ordinary differential equations that can be solved numerically (Elliott et al., 2007; Liu and Neely, 2010; Teal et al., 2011). The differential equations can also be derived by equivalent circuits for the nonelectrical parts of the model. Representing the proposed model with equivalent electrical circuits provides access to numerous powerful tools that have been designed for circuit analysis. The equivalent electrical circuits of the proposed model are represented in Appendix B.

Fig. IV illustrates the time domain analysis for two different positions along the cochlea for stable system including nonlinearity in the MET channel current.

### A. Spontaneous Cochlear Microphonic

The origin of SOAE presumably is preexisting mechanical perturbations (Manley and Fay, 2008) which can be considered the source of rapid change in cochlear amplifier gain for some places along the cochlea (Elliott et al., 2007; Ku et al., 2008).

It has been shown (Neely and Kim, 1986) that the cochlear amplifier gain ($\gamma$) is responsible

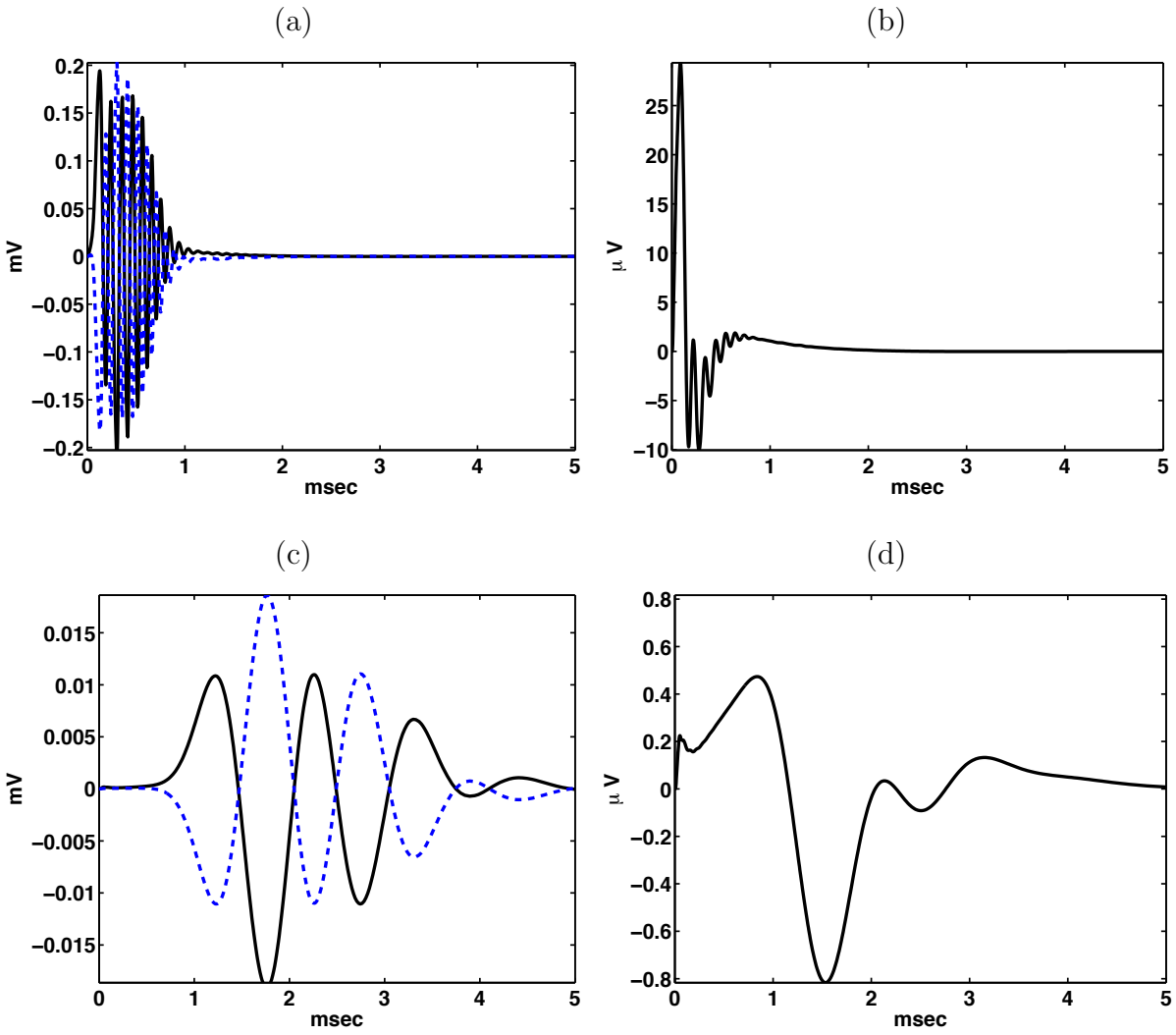


FIG. 6. $V_{\mathrm{HB}}$, $V_{\mathrm{OHC}}$ and CM for two different positions along the cochlea. (a) and (c) show $V_{\mathrm{HB}}$ (solid line) and $V_{\mathrm{OHC}}$ (dash line) for 5mm and 20mm from the base respectively. (b) and (d) show the CM for 5mm and 20mm from the base respectively.

for the sharpness of the tuning curve of basilar membrane displacement. If it is assumed that $\gamma$ is fixed and independent of position along the cochlea, increasing the cochlear amplifier gain can make the (linear) cochlear model unstable. Different assumptions about ways in which $\gamma$ can vary along the cochlea have been explored (Elliott et al., 2007; Ku et al., 2008) and it has been shown that introducing instability to the model by rapid change of $\gamma$ agrees with previous conjectures about SOAEs (Zweig and Shera, 1995).

(a)

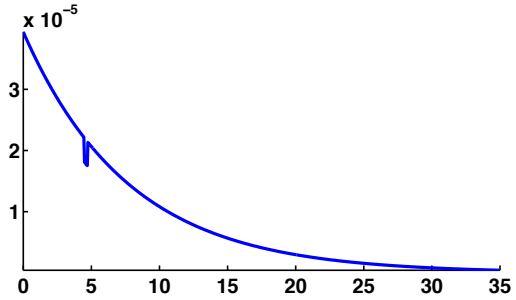


(b)

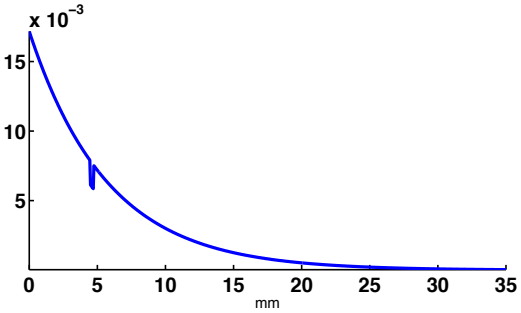


FIG. 7. (a) illustrates perturbations in $\alpha_{\mathrm{v}}$ (b) illustrates perturbations in $\alpha_{\mathrm{d}}$. In (a) and (b), the preexisting mechanical perturbations assumed to occur about 5mm from the stapes

In the proposed model , the cochlear amplifier gain is determined by $\alpha_{\mathrm{v}}$ and $\alpha_{\mathrm{d}}$ (see Fig. 2). Fig. 7 depicts an idealised small perturbations along the cochlea. Fig. 3 shows the effect of these perturbations on the root locations for the linearised version of the model.
Fig. 8 shows their effect on the behaviour of the basilar membrane velocity and of the CM. Preexisting mechanical perturbations cause oscillation in the basilar membrane which can be detected in the ear canal as SOAEs. Analogously these perturbations also produce Spontaneous Cochlear Microphonic (SCOMIC).

## V. CONCLUSIONS

The CM is an electrical signal which has not received enough attention since its discovery eighty years ago. This signal can be used as a valuable tool for studying the hearing mech-

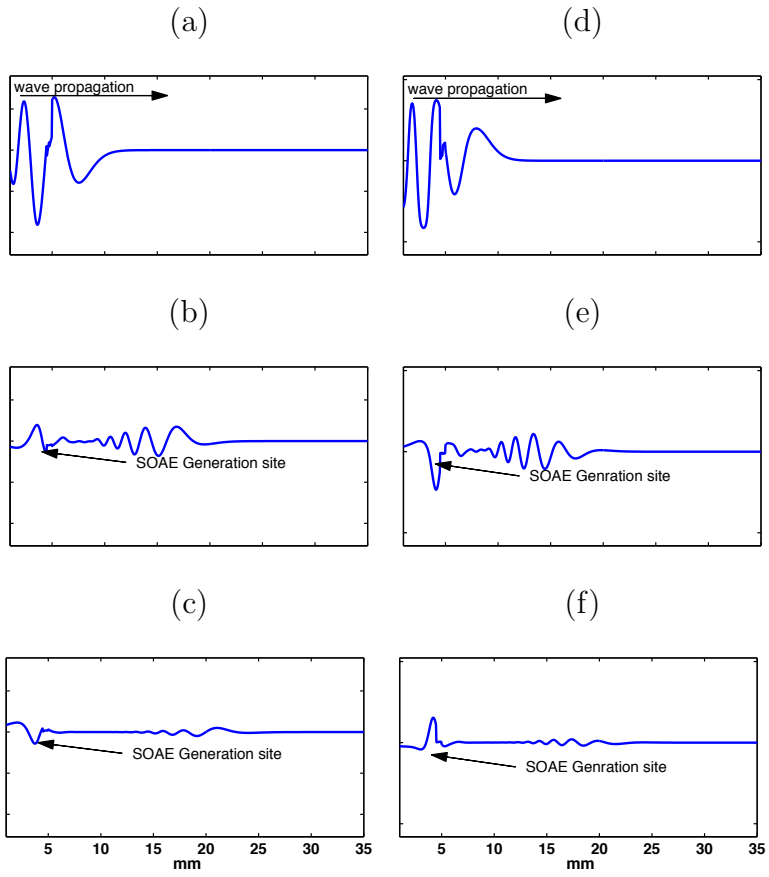


FIG. 8. (a), (b) and (c) show how the step stimulus wave propagates in the basilar membrane along the cochlea for $t = 0.2$, $t = 1$ and $t = 2$ msec respectively. (d), (e) and (f) show how the CM wave propagates in the basilar membrane along the cochlea for $t = 0.2$, $t = 1$ and $t = 2$ msec respectively. Time domain analysis of nonlinear cochlear model indicates that in addition to SOAEs; preexisting mechanical perturbations produce Spontaneous Cochlear Microphonic (SCOMIC) too.

anism as well as having other possible clinical applications. By modelling the mechanisms which are involved in generating this signal, the physiological understanding of cochlear function can be examined and extended.

In this research, an integrated mechano-electrical model of the human hearing system is proposed. The results of the proposed model have shown that small rapid perturbations in feedback gain which have been previously hypothesised to be the generation source of

SOAEs can generate Spontaneous Cochlear Microphonic (SCOMIC) as well. Even though this signal has not yet been reported, it could play important role in auditory research. Actual recording of this signal can show whether previous hypotheses about the generation source of SOAE are valid or should be amended to explain this phenomenon. The existence of SCOMIC can also provide a better understanding of the main sources of active processes inside the cochlea.

In this paper, by using circuit equivalents for non-electrical parts; the entire model has been represented as an electrical circuit. Using electrical circuit analysis software all potentials of electrical network of the organ of Corti can be readily accessed. The results of examining potentials of the OHC and the organ of Corti of the model have shown that the sharpness difference between the basilar membrane velocity and the CM is the result of the phase difference between the hair bundle potential and the OHC potential.

The results of the proposed model agree with previous physiologically measurable parameters and outcomes of other similar models. This research can be extended by attempting to determine the existence or non-existence of SCOMIC and also by interpreting the CM signal produced by a hearing system having impaired OHCs. The combination of CM, audiograms and otoacoustic emissions may help audiologist to distinguish OHC hearing loss (Sensitivity loss) or inner hair cells loss (Clarity loss)(Killion and Niquette, 2000) for prescribing suitable hearing aids or treatments.

## APPENDIX A: STATE SPACE FORMULATION

The dynamic behaviours of the proposed model can be explored by the state-space representation of the model. For evaluating stability, the linearised version has been used. The state matrix $\mathbf{A}$ which has been introduced in Section II.A.1 can be written as the sum of four matrices that correspond to the middle ear and the earphone diaphragm $\mathbf{A}_{\mathrm{ME}}$, micromechanics $\mathbf{A}_{\mathrm{C}}$, electrical coupling $\mathbf{A}_{\mathrm{G}}$ and pressures $\mathbf{A}_{\mathrm{P}}$. The first six elements of state vector $\mathbf{x}$ are $[x_{\mathrm{d}}, v_{\mathrm{d}}]$ which represent the displacement and velocity of the earphone

diaphragm (Liu and Neely, 2010) and [$x_{\mathrm{m}}$, $v_{\mathrm{m}}$, $x_{\mathrm{s}}$, $v_{\mathrm{s}}$] which represent the displacement and velocity of the malleus-incus and stapes-eardrum system (see Fig. 1 (a) and (b)). The first six rows and six columns of $\mathbf{A}_{\mathrm{ME}}$ are the coefficients of these state variables after writing equilibrium equations for different parts of Fig. 1 (a) and (b) and all other elements of this matrix are zeros.

Combining the derivative of equation (1) with $\dot{\xi}_{\mathrm{r}} = \partial\xi_{\mathrm{r}}/\partial t$ and with the equilibrium equations Fig. 1(d) results in $4 \times N$ state equations which can be used to construct matrix $\mathbf{A}_{\mathrm{C}}$. The equations related to the velocity of RL ($\dot{\xi}_{\mathrm{r}}$) also include $P$ (Fluid pressure).

Fluid pressure acting on the basilar membrane (see Fig. 1 (C)) can be expressed in terms of other state variables. The following equations govern cochlear macromechanics:

$$\partial_x P = -\frac{\rho}{A}\partial_t U \tag{A1}$$

$$\partial_x U = w\dot{\xi}_{\mathrm{r}} \tag{A2}$$

where $P$ denotes the pressure difference between the two cochlear chambers (scala vestibuli and scala tympani), $x$ denotes the longitudinal direction from the base to the apex, $\rho$ denotes the effective fluid mass density, $A$ denotes the cross-sectional area of the fluid chamber, and $U$ denotes the volume velocity along the $x$-direction. $w$ is the width of the basilar membrane. The boundary conditions for the equation (A1) are:

$$\partial_x P|_{x=0} = -\rho\dot{v}_{\mathrm{s}} \tag{A3}$$

$$\partial_x P|_{x=L} = \frac{-\rho}{Am_{\mathrm{h}}}P(L) \tag{A4}$$

where $m_{\mathrm{h}}$ represents the mass of the fluid at the helicotrema (refer to (Liu and Neely, 2010) for more details). By combining equations (A1) and (A2) and ignoring the derivative term of cross-sectional area, the pressure can be modelled as follows:

$$\partial_x^2 P = -\frac{\rho}{A}w\partial_t^2\xi_{\mathrm{r}} \tag{A5}$$

By using the finite differential method, and appropriate boundary conditions at the base and apex ( equations (A3) and (A4) ) and the equilibrium equation for the micromechanical

part of the model ( see Fig. 1 (d) ), equation (A5) can be rewritten in matrix form as:

$$\left(\mathbf{D}_2 - \text{Diagonal}(\frac{\rho}{A}w)\right)\, P = \mathbf{LX} \tag{A6}$$

Where $\mathbf{D}_2$ is an $N \times N$ tridiagonal centered finite difference approximation matrix with appropriate boundary conditions at the base and apex. Pressure $P(x)$ only appears in state equations related to the velocity of RL $\dot{\xi}_{\text{r}}$, so a coefficient matrix $P_{\dot{\xi}_{\text{r}}}$ is required to rearrange pressure values to suitable matrix format. Therefore:

$$\mathbf{A}_{\text{P}} = P_{\dot{\xi}_{\text{r}}}\, \left(\mathbf{D}_2 - \text{Diagonal}(\frac{\rho}{A}w)\right)^{-1} \mathbf{L} \tag{A7}$$

For obtaining equations related to OHC and hair bundle voltages nodal analyses have been used. Using Kirchhoff's laws for each node in electrical model (Fig. 2) results in the following equation:

$$\mathbf{GV} = \mathbf{EX} \tag{A8}$$

where

$$V = [V_{\text{st}}(1)\, V_{\text{sm}}(1)\, V_{\text{sv}}(1)\, \dot{V}_{\text{OHC}}(1)\, \dot{V}_{\text{HB}}(1)\ \cdots\ \dot{V}_{\text{HB}}(N)]^{\top}$$

the right side of equation (A8) is made up of a combination of $V_{\text{OHC}}$, $V_{\text{HB}}$, $i_{\text{r}}$ and $i_{\text{Q}}$ in each row and this combination can be written as $\mathbf{EX}$. It is worth mentioning that $I(\eta) \simeq \eta$ has been used for linearisation (see the caption of Fig. 2 and (Liu and Neely, 2010)).
Matrix $\mathbf{K}$ can be made to extract $2 \times N$ equations related to state variables $\dot{V}_{\text{OHC}}$ and $\dot{V}_{\text{HB}}$. Therefore:

$$\mathbf{A}_{\text{G}} = \mathbf{K}\, \mathbf{G}^{-1}\mathbf{E} \tag{A9}$$

and finally

$$\mathbf{A} = \mathbf{A}_{\text{ME}} + \mathbf{A}_{\text{C}} + \mathbf{A}_{\text{P}} + \mathbf{A}_{\text{G}} \tag{A10}$$

## APPENDIX B: EQUIVALENT ELECTRICAL CIRCUIT

The analogy between simple mechanical and electrical systems is straightforward (Senturia, 2001). Consider the mechanical system in Fig. 9. Newton's second law mandates the following equation:

$$F = Kx + M\frac{d^2x}{dt^2} + B\frac{dx}{dt} \tag{B1}$$

By using Kirchhoff's current and voltage laws for the electrical circuit in Fig. 9 the following equation can be written:

$$V = \frac{1}{C}\int_0^t idt + L\frac{di}{dt} + Ri \tag{B2}$$

If we assume that the velocity $\dot{x}$ is equivalent to the electrical current $i$ (the velocity and


FIG. 9. A mechanical system and its equivalent electrical circuit. $i$ represents the electrical current in the electrical system and $x$ represents the displacement. By taking the velocity $\dot{x}$ equivalent to the electrical current $i$, and appropriate values for each component in both the electrical circuit and the mechanical system, the output for both will be identical.

current goes through a series of elements and are called *through variables*), the force $f$ is equivalent to the voltage $v$ (the force and voltage are called *across variables*). We can represent these equivalents as $\dot{x} \Leftrightarrow i$ and $f \Leftrightarrow v$. Using this notion, $B \Leftrightarrow R$, $M \Leftrightarrow L$ and $K \Leftrightarrow 1/C$. The differential equations (B1) and (B2) are equivalent and the mechanical system and electrical circuit in Fig. 9 become equivalent (see (Senturia, 2001) for other examples). This analogy can be extended to acoustic and fluid systems.

## 1. Equivalent Circuit of the Sound Source and Middle Ear Models

The models of the sound source and middle ear are composed of simple acoustical and mechanical components which can be converted to equivalent circuits by exploiting the approach of the previous section. Those models also include lever gains and the pressures on changing cross sectional areas both of which can be represented by ideal transformers. Fig. 10 demonstrates the equivalent circuit for this part of the model.

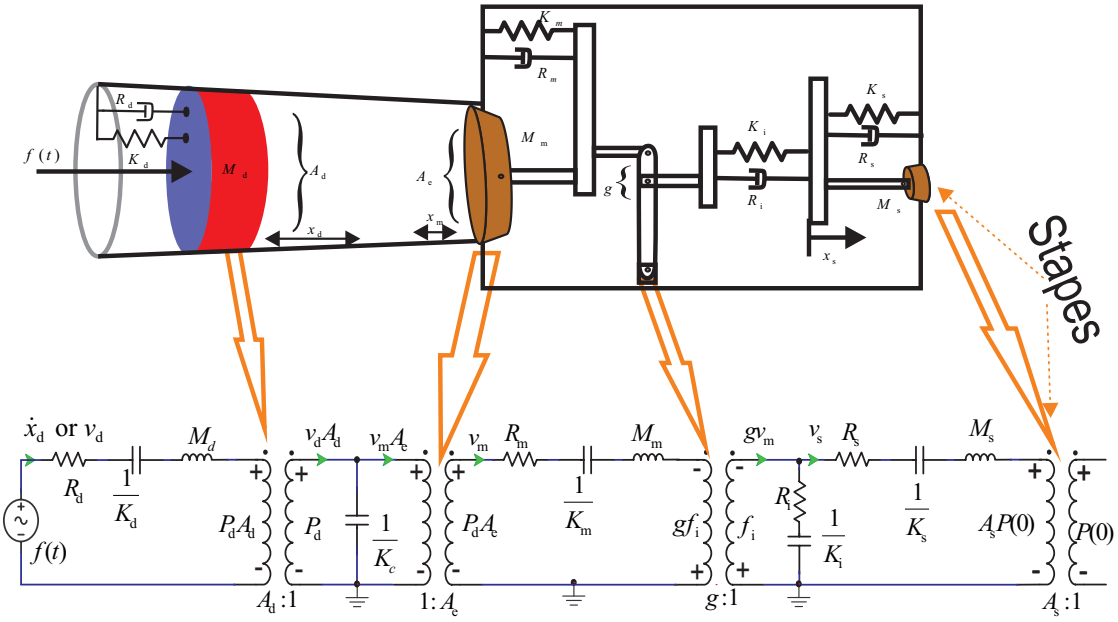


FIG. 10. Equivalent circuit of the sound source and middle ear models

## 2. Equivalent Circuit of Cochlear Macromechanics

By writing the finite difference approximation for (A1) and (A2), the following equations are derived:

$$\frac{P(i)-P(i-1)}{\Delta x} = -\frac{\rho}{A(i)}\partial_t U \tag{B3}$$

$$\frac{U(i+1)-U(i)}{\Delta x} = w\dot{\xi}_{\mathrm{r}} \tag{B4}$$

The fluid velocity is equivalent to the current and the fluid pressure is equivalent to the voltage, so (B3) represents an inductor in the circuit equivalent, with the inductance $L(i) = \frac{\rho}{A(i)}\Delta x$. By using same approach, (A3) represents an inductor with the inductance $\acute{L} = \frac{\rho}{A_{\mathrm{s}}}\Delta x$ and (A4) represents two resistors at the helicotrema with resistances $R_1 = \frac{\rho}{A(N-1)m_{\mathrm{h}}}$ and $R_2 = \frac{1}{\Delta x}$.

### 3. Equivalent Circuit of Cochlear Micromechanics

The components of the circuit equivalent for cochlear micromechanics are presented in Fig. B.3. Equation (B4) dictates that the current in the branch $i$ should be $w\Delta x\dot{\xi}_{\mathrm{r}}$, therefore, the electrical component values in the basilar membrane and OHC branches are adjusted to meet this requirement. By considering equation (2), the dependent voltage source $f_{\mathrm{OHC}}$ relies on $Q$ and $V_{\mathrm{OHC}}$. $Q$ can be obtained by equation (1). This procedure can be accomplished by using a dependent current source and a capacitor in the circuit equivalent (see Fig. B.3). $V_{\mathrm{OHC}}(i)$ is the electrical potential of $R_4(i)$ in the potential coupling (see Fig. 2). $i_{\mathrm{r}}(i)$ depends on the displacement and velocity of the reticular lamina. $\dot{\xi}_{\mathrm{r}}$ can be obtained by using the current of the basilar membrane and OHC branches. $\xi_{\mathrm{r}}$ can be calculated by a dependent current source and a capacitor in the circuit equivalent (see Fig. B.3). Therefore, $\eta = \alpha_{\mathrm{v}}\dot{\xi}_{\mathrm{r}}(i) + V_i$.

The circuit representation of the model can be easily implemented in circuit analysis software[3]

## APPENDIX C: PARAMETER SELECTION

The parameters of the model vary with longitudinal position. Greenwood's frequency-place map constrains most of the parameters to be exponentially dependent on the distance from the base (Liberman, 1982; Greenwood, 1990). In current work, the mechanical parameter values, have been taken from (Liu and Neely, 2010). However for agreement with new measurements of electrical parameters (Johnson et al., 2011), some of parameters are

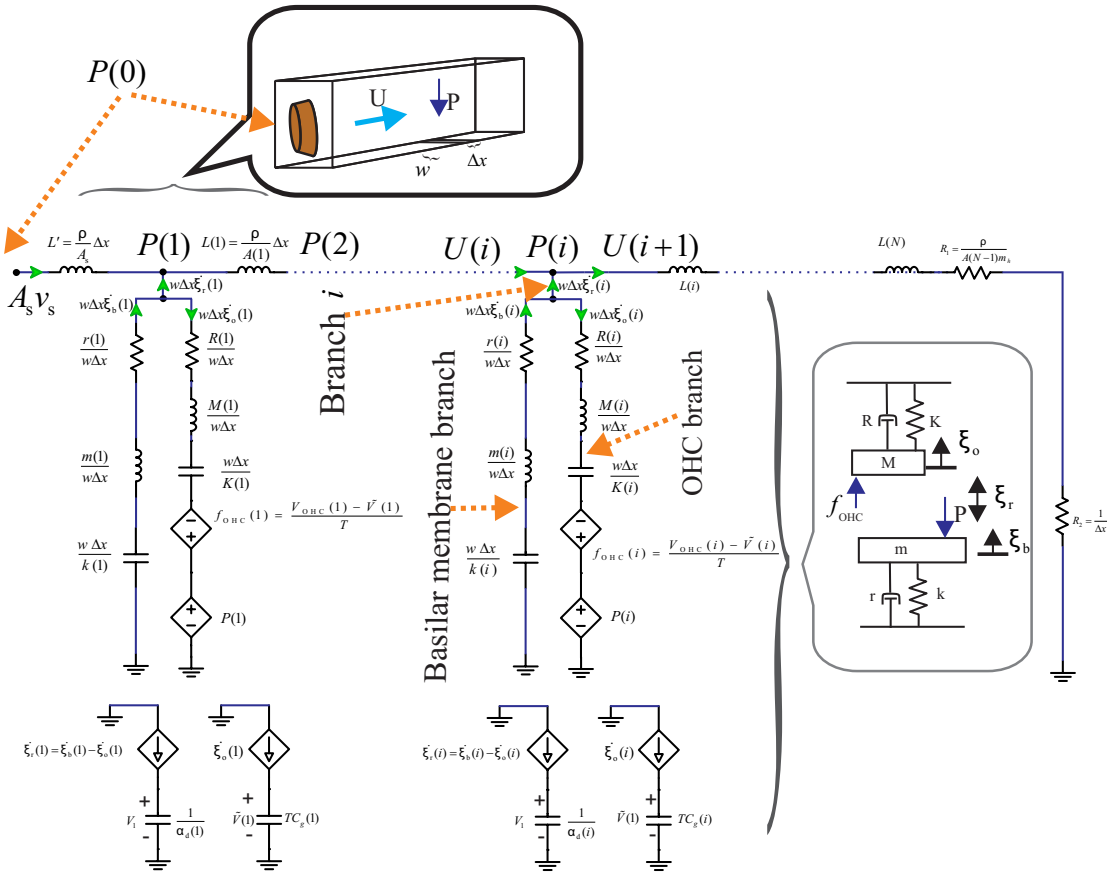


FIG. 11. Equivalent circuit of the cochlea (cochlear macromechanics and micromechanics), $V_i = \alpha_{\rm d}\xi_{\rm r}(i)$ and $Q(x) = (T)^{-1}\xi_o(x)$.

revised and are listed in table I.

## ENDNOTES

1. Note the antisymmetric form of the equation based on (Johnson et al., 2011) has been used.

2. For simplicity, although a linearised version of the model has been represented here some of the following results retain the nonlinear form.

3. For this purpose, LTspice free SPICE software from Linear Technology Corporation has been used( http://www.linear.com/designtools/software/).

## REFERENCES


J. Ashmore, P. Avan, W. Brownell, P. Dallos, K. Dierkes, R. Fettiplace, K. Grosh, C. Hackney, A. Hudspeth, and F. Jlicher. The remarkable cochlear amplifier. *Hearing Research*, 266 (1):1–17, 2010.

M. Cheatham, K. Naik, and P. Dallos. Using the cochlear microphonic as a tool to evaluate cochlear function in mouse models of hearing. *JARO-Journal of the Association for Research in Otolaryngology*, 12:113–125, 2011.

P. Dallos. Some electrical circuit properties of the organ of Corti. i. analysis without reactive elements. *Hearing Research*, 12:89–119, 1983.

P. Dallos. Some electrical circuit properties of the organ of Corti. ii. analysis including reactive elements. *Hearing Research*, 14:281–291, 1984.

P. Dallos, A. Popper, and R. Fay, editors. *The Cochlea*. Springer Handbook of Auditory Research. Springer, 1996.

H. Davis. A model for transducer action in the cochlea. *Cold Spring Harbor symposia on quantitative biology*, 30:181–190, 1965.

S. Elliott, E. Ku, and B. Lineton. A state space model for cochlear mechanics. *The Journal of the Acoustical Society of America*, 122(5):2759, 2007.

S. A. Gelfand. *Hearing: An Introduction to Psychological and Physiological Acoustics*. Informa Healthcare, 2010.

D. Greenwood. A cochlear frequency-position function for several species29 years later. *The Journal of the Acoustical Society of America*, 87:2592, 1990.

S. Iurato. Functional implications of the nature and submicroscopic structure of the tectorial and basilar membranes. *The Journal of the Acoustical Society of America*, 34(9B):1386–1395, 1962.

S. L. Johnson, M. Beurg, W. Marcotti, and R. Fettiplace. Prestin-driven cochlear amplification is not limited by the outer hair cell membrane time constant. *Neuron, Elsevier*, 70 (6):1143–1154, 2011.

H. Kennedy, A. Crawford, and R. Fettiplace. Force generation by mammalian hair bundles supports a role in cochlear amplification. *Nature*, 433:880–883, 2005.

M. Killion and P. Niquette. What can the pure-tone audiogram tell us about a patients snr loss. *Hear J*, 53(3):46–53, 2000.

E. Ku, S. Elliott, and B. Lineton. Statistics of instabilities in a state space model of the human cochlea. *The Journal of the Acoustical Society of America*, 124:1068, 2008.

M. C. Liberman. The cochlear frequency map for the cat: Labeling auditory-nerve fibers of known characteristic frequency. *The Journal of the Acoustical Society of America*, 72(5): 1441–1449, 1982.

Y.-W. Liu and S. T. Neely. Outer hair cell electromechanical properties in a nonlinear piezoelectric model. *The Journal of the Acoustical Society of America*, 126(2), 2009.

Y.-W. Liu and S. T. Neely. Distortion product emissions from a cochlear model with nonlinear mechanoelectrical transduction in outer hair cells. *The Journal of the Acoustical Society of America*, 127(4), 2010.

G. Manley and R. Fay. *Active processes and otoacoustic emissions in hearing*, volume 30. Springer, 2008.

A. Masood, P. Teal, and C. Hollitt. A non-invasive cochlear microphonic measurement system. *Medical Engineering & Physics*, 2012.

P. Mistrík, C. Mullaley, F. Mammano, and J. Ashmore. Three-dimensional current flow in a large-scale model of the cochlea and the mechanism of amplification of sound. *Journal of The Royal Society Interface*, 6:279–291, 2009.

S. T. Neely and D. O. Kim. A model for active elements in cochlear biomechanics. *The Journal of the Acoustical Society of America*, 79(5):1472–80, 1986.

J. O. Pickles. *An Introduction To The Physiology Of Hearing*. Emerald Group Publishing, third edition, 2008.

J. Poch-Broto, F. Carricondo, B. Bhathal, M. Iglesias, J. Lpez-Moya, F. Rodrguez, J. Sanjun, and P. Gil-Loyzaga. Cochlear microphonic audiometry: a new hearing test for objective diagnosis of deafness. *Acta oto-laryngologica*, 129(7):749–754, 2009.

S. Ramamoorthy, N. V. Deob, and K. Grosh. A mechano-electro-acoustical model for the cochlea: Response to acoustic stimuli. *The Journal of the Acoustical Society of America*, 121(5):2758–2773, 2007.

S. Senturia. *Microsystem Design*. Springer Netherlands, 2001.

D. Strelioff. A computer simulation of the generation and distribution of cochlear potentials. *The Journal of the Acoustical Society of America*, 54(3):620–9, 1973.

P. Teal, B. Lineton, and S. Elliott. An electromechanical model for the cochlear microphonic. In *AIP Conf. Proc*, volume 1403, pages 652–657, 2011.

G. Zweig and C. Shera. The origin of periodicity in the spectrum of evoked otoacoustic emissions. *The Journal of the Acoustical Society of America*, 98:2018, 1995.

TABLE I. Parameters used in the model.

| Property | meaning (Unit) | Base | Apex | reference |
|---|---|---|---|---|
| $T$ | Piezoelectric transformer ratio (m/C) | $2.7 \times 10^6$ | $2.8 \times 10^6$ | Estimated [a] |
| $\alpha_{\mathrm{d}}$ | MET current's sensitivity to RL displacement (A/m) | $1.7 \times 10^{-2}$ | $3.8 \times 10^{-5}$ | Estimated [a] |
| $\alpha_{\mathrm{v}}$ | MET current's sensitivity to RL velocity (C/m) | $3.95 \times 10^{-5}$ | $4.3 \times 10^{-7}$ | Estimated [a] |
| $C_4$ | Membrane basolateral capacitances (nF/m) | 360 | 4200 | Estimated [b] |
| $C_3$ | Membrane apical capacitances (nF/m) | 72 | 840 | Estimated [c] |
| $R_1$ | The impedances between SL and SV ($\Omega$m) | 10 | 10 | Based on [d] |
| $R_2$ | The impedances between SV and SM ($\Omega$m) | 25 | 25 | Based on [d] |
| $R_3$ | The membrane impedances of the hair bundle ($\Omega$m) | 170 | 340 | Estimated [b] |
| $R_4$ | The membrane impedances of the OHCs ($\Omega$m) | 55 | 300 | Estimated [b] |
| $R_5$ | The impedances between ST and SL ($\Omega$m) | 25 | 25 | Based on [d] |
| $R_6$ | The impedances between SV and SM ($\Omega$m) | 27 | 27 | Based on [e] |
| $R_8$ | The longitudinal resistors along the cochlea (M$\Omega$/m) | 3 | 3 | Based on [d] |
| $R_9$ | The longitudinal resistors along the cochlea (M$\Omega$/m) | 5 | 5 | Based on [d] |
| $R_{11}$ | The longitudinal resistor along the cochlea (K$\Omega$/m) | 150 | 150 | Based on [d] |

[a]Estimated based on Liu and Neely (2010) and agreement with Greenwood's function.

[b]Estimated based on Johnson et al. (2011) and agreement with Greenwood's function.

[c]The membrane area of rat OHCs and the area of their hair bundles indicate $C_3/C_4 = 0.2$ independent of the location along the cochlea (Johnson et al., 2011), and we assumed the ratio is true for human OHCs.

[d]Ramamoorthy et al. (2007) note: the spiral ligament (SL) has been considered as electrical ground (0V)

[e]Strelioff (1973)

## LIST OF FIGURES